Dusp-5 and Snrk-1 coordinately function during vascular development and disease

*Kallal Pramanik,[1] *Chang Zoon Chun,[1] *Maija K. Garnaas,[1] Ganesh V. Samant,[1] Keguo Li,[1] Mark A. Horswill,[1] Paula E. North,[2] and Ramani Ramchandran[1,2]

[1]Department of Pediatrics, Children's Research Institute (CRI) Developmental Vascular Biology Program, and [2]Department of Pediatric Pathology, Translational and Biomedical Research Center, Medical College of Wisconsin, Milwaukee

Mitogen-activated protein kinases play an integral role in several cellular processes. To regulate mitogen-activated protein kinases, cells express members of a counteracting group of proteins called phosphatases. In this study, we have identified a specific role that one member of this family of phosphatases, dual-specific phosphatase-5 (Dusp-5) plays in vascular development in vivo. We have determined that *dusp-5* is expressed in angioblasts and in established vasculature and that it counteracts the function of a serine threonine kinase, Snrk-1, which also plays a functional role in angioblast development. Together, Dusp-5 and Snrk-1 control angioblast populations in the lateral plate mesoderm with Dusp-5 functioning downstream of Snrk-1. Importantly, mutations in *dusp-5* and *snrk-1* have been identified in affected tissues of patients with vascular anomalies, implicating the Snrk-1–Dusp-5 signaling pathway in human disease. (Blood. 2009;113: 1184-1191)

Introduction

The mitogen-activated protein kinase (MAPK) pathway[1] represent a key signal integration step inside the cell for various extracellular stimuli.[2] At least 4 MAPK families have been identified: the extracellular signal-regulated kinases 1 and 2 (ERK1/2), c-Jun N-terminal kinase (JNK), p38, and Erk5. Each MAPK is activated by specific MAPK kinases (Mkks or Meks), which in turn are regulated by Mek kinases (Mekks). To date, several members of the MAPK family, including Erk5[3] and Mekk3,[4] have been implicated in vascular development in vivo.[5] Furthermore, MAPKs are often associated with pathologic responses, such as stress, apoptosis, inflammation, and cell proliferation.[5,6] In terms of vascular conditions, differential expression of active MAPKs was noticed in several types of hemangiomas,[7] the most common vascular tumor of infancy and childhood,[8] and the presence of immunoreactive phosphorylated MAPK inversely correlate with degree of malignancy.[7] Therefore, from a drug discovery standpoint, vascular specific components of MAPKs cascade are promising drug targets.[6]

MAPKs are activated by dual phosphorylation of tyrosine and threonine residues in their activation loops. To control MAPK activation, a family of proteins called dual-specificity protein tyrosine phosphatases (DUSPs) dephosphorylate both residues.[9] DUSPs come in 2 varieties: dual-specificity MAPK phosphatases and atypical DUSPs. A dual specific phosphatase, Dusp-5, was recently identified by 2 independent microarray studies as a vascular-specific gene,[10,11] and we hypothesized that dusp-5 plays a specific role in vascular development. To investigate dusp-5 function, we initiated a loss-of-function (LOF) study in zebrafish (ZF). We identified that dusp-5 LOF embryos showed enhanced *etsrp*[+] angioblasts at the lateral plate mesoderm (LPM). Recently, we had identified in a gain-of-function (GOF) and LOF study for a serine-threonine kinase member of the sucrose nonferminting kinase family, Snrk-1, that it increased or decreased, respectively, the same *etsrp*[+] angioblast population at the LPM.[12] Taking these findings together, we hypothesized that, during vascular development, Dusp-5 and Snrk-1 function together in controlling angioblast numbers at the LPM. In this study, we show that *dusp-5* is expressed in angioblasts in the embryonic ZF and is essential for vascular development in vivo. We show that loss of Dusp-5 function in vitro causes apoptosis of endothelial cells (ECs), and Dusp-5 and Snrk-1 target a common signaling pathway responsible for maintaining angioblast populations along the LPM. Snrk-1 ectopically induces *etsrp*[+] angioblasts in the LPM, which is blocked by Dusp-5 that functions downstream of Snrk-1. In addition, we have identified mutations in *dusp-5* and *snrk-1* in the lesional tissue of many vascular anomaly patient samples, suggesting a critical role for this pathway in disease.

Methods

ZF stocks

Wild-type ZF (TuAB strain) were grown and maintained at 28.5°C.[13] All procedures were performed according to animal protocol guidelines (ASP no. 312-06-2) set by the Medical College of Wisconsin (Milwaukee). Mating was routinely carried out at 28.5°C, and the embryos were staged according to established protocols.[14]

Microinjections

Microinjections of 1-cell stage ZF embryos with RNA or morpholinos (MOs) were carried out as described before.[13] MOs were reconstituted in nuclease-free water to 2-mM stock concentration (16 ng/nL). Appropriate

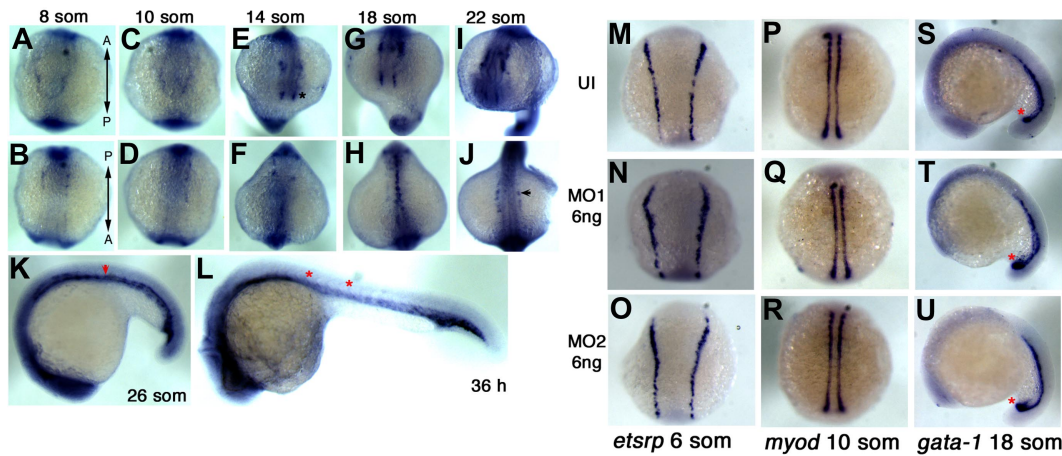The online version of this article contains a data supplement.

Figure 1. Whole-mount ISH expression pattern of *dusp-5* and effect of in vivo knockdown of *dusp-5* on *etsrp*$^+$ cells in the ZF embryo. (A-L) Whole-mount ISH using *dusp-5* antisense probes, with the embryo stages depicted on top of or inside each panel. (A,C,E,G,I) Top panels: Top views of the anterior embryo regions. (B,D,F,H,J) Dorsal views of the head and trunk regions. (K,L) Lateral views of the embryo with the head to the left. (M-O) *etsrp*, 6 som, (P-R) *myod*, 10 som, and (S-U) *gata-1*, 18 som show ISH embryos stained for indicated markers. (M,P,S) UI embryos. (N,Q,T) 6 ng of MO1-injected. (O,R,M) 6 ng of MO2 injected embryos. "A" and "P" labels denote the direction of the anterior-posterior axis in panels A and B. Black asterisk in panel E indicates head *dusp-5*$^+$ populations; arrowhead in panel J, *dusp-5*$^+$ angioblasts in LPM; red asterisks in panel K, *dusp-5*$^+$ angioblasts coalescing to form axial vessels, in panel L (intersomitic vessels) and in panels S to U (*gata-1*$^+$ cells in blood islands).

dilutions were made in 5× injection dye (100 mM *N*-2-hydroxyethylpipera-zine-*N′*-2-ethanesulfonic acid, 1 M KCl, 1% phenol red) and approximately 2 to 3 nL MOs (6-18 ng) were injected at the 1-cell stage. RNA overexpression was performed with 75 pg of capped sense RNA generated from a *Sca*I-linearized template, pBluescriptII-SNRK-1, and pBluescript SK-DUSP-5 (Open Biosystems, Huntsville, AL), using T3 RNA polymerase. In the double injection experiments, 6 ng of dusp-5 MO or snrk-1 MO and 75 pg of capped sense mRNA were combined together and injected into 1-cell stage embryo.

dusp-5 siRNA knockdown

The human *dusp-5* region corresponding to bps 406 to 854 was amplified using primers: forward, TATCCTGAGTGTTGCGTGGA; reverse, CG-GAACTGCTTGGTCTTCAT. The siRNA was generated according to BLOCK-iT Complete Dicer RNAi Kit (Invitrogen, Carlsbad, CA) recom-mendations. Human umbilical vein endothelial cell (HUVECs) were grown to 70% confluence and transiently transfected with 100 ng of small-interfering RNA (siRNA) per 100-mm plate by Lipofectamine 2000 Reagent (Invitrogen).

Whole-mount in situ hybridization and probes

Whole-mount in situ hybridization (ISH) was carried out as described before.[15] For antisense RNA probe generation for ZF *dusp-5*, template was generated by polymerase chain reaction (PCR) using the forward and reverse primers containing T7 and T3 promoter sequence. The primer sequences were: forward, TAATACGACTCACTATAGGGATGAAG-GTCTCCAGCATAGATTG; and reverse, ATTAACCCTCACTAAAGG-GATTAAGGCAGCGCAGTTATTG. Transcription was performed with T3 RNA polymerase in the presence of digoxigenin-labeled deoxyribonucleo-side triphosphate to generate an antisense RNA probe against *dusp-5*. Probes for *fli*, *ephrin-B2a*, *flt-4*, and *grl* have been described before.[16-18] *etsrp* cDNA was a kind gift from Dr Saulius Sumanas (University of California–Los Angeles). Hybridized embryos were photographed using a Leica stereomicroscope (Wetzlar, Germany) equipped with a Qimaging camera and Image Pro AMS 6.0 software. All images were taken with embryos mounted in glycerol as described before[15] and images assembled in Adobe Photoshop elements program (Adobe Systems, Mountain View, CA).

Human patient samples

Research on human patient samples were performed according to Medical College of Wisconsin–approved Institutional Review Board protocols, and informed consent was obtained in accordance with the Declaration of Helsinki.

Results

Characterization and expression of ZF *dusp-5*

ZF Dusp-5 is 61.2% and 60.7% identical (Figure S1A, available on the *Blood* website; see the Supplemental Materials link at the top of the online article) to human and mouse Dusp-5 proteins, respec-tively. The ZF protein contains a Rhodanese-like domain (11-134 AA), dual-specific phosphatase catalytic domain (170-308 AA), and a tyrosine-specific phosphatase active site (253-265 AA), all of which is conserved in human and mouse. Based on the current ZF genome assembly, *dusp-5* is located on linkage group 22 and spans 5 exons and 4 introns in the genome.

A whole-mount ISH expression profile of *dusp-5* has been reported previously by Sumanas et al, at selected stages in ZF development.[11] We expanded the ISH data by including additional time points between 3 somite and 26 hours postfertilization and thereby conclusively demonstrated that *dusp-5* is expressed in developing vasculature during embryonic ZF development. We confirm the results of Sumanas et al,[11] that starting at 3 som, *dusp-5* is expressed in angioblasts emerging from the LPM and further show that at 8 and 10 som, *dusp-5*$^+$ cells appear in the head and trunk region (Figure 1A-D). At 14 som, *dusp-5*$^+$ cells form 4 clusters in the head (Figure 1E black asterisk) that resemble clusters of *etsrp*$^+$ cells. In the 14 som trunk, *dusp-5*$^+$ cells are located in the midline (Figure 1F) where they coalesce in an anterior to posterior direction by 18 som (Figure 1H). Some angioblasts remain behind in 22 som embryos (Figure 1J black arrow) and by 26 som, *dusp-5* is expressed in the dorsal aorta (DA) and posterior cardinal vein (PCV; Figure 1K). At 36 hpf, *dusp-5*$^+$ intersomitic vessels sprout from the DA (Figure 1L red asterisk). These results confirm that *dusp-5* is expressed in the developing vasculature in vertebrates.

Dusp-5 loss of function in vivo alters *etsrp*$^+$ angioblast populations

To investigate *dusp-5* function during embryonic ZF develop-ment, we designed 2 MOs. MO1 targets the exon 2–intron 2 splice junction, whereas MO2 targets the ATG in the 5′UTR of
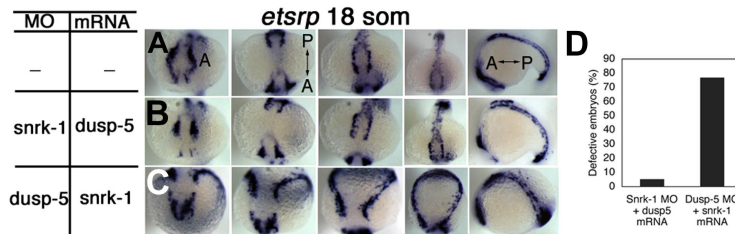
Figure 2. Snrk-1 and *dusp-5* interact functionally in a single direction affecting *etsrp*+ cell populations and their migration to the midline. (A) Whole-mount ISH expression pattern of *etsrp*+ cells in WT embryos. In the *snrk-1* MO plus dusp-5 mRNA background (B), *etsrp*+ cells appear in similar locations and pattern normally compared with age-matched WT embryos (A). In the *dusp-5* MO plus *snrk-1* mRNA background (C), *etsrp*+ cells do not migrate to the midline, and a gross increase in this population occurs in the LPM. (D) Quantification of the percentage of embryos displaying defects observed in panels B (n = 38) and C (n = 26). "A" and "P" labels denote the direction of the anterior-posterior axis in panel A and corresponding panels. The MO doses were 6 ng, and the mRNA dose was 75 pg.

the *dusp-5* transcript (Figure S1B). Initially, we performed a dose curve for dusp-5 MOs and performed reverse-transcribed PCR (RT-PCR) across exons 1 to 4. At 6 ng of dusp-5 MO, we observed that the *dusp-5* transcript is reduced in MO1-injected 24 hpf embryos (Figure S1C lanes MO1) compared with uninjected (UI) embryos (Figure S1C lane UI). As the concentration of MO1 was increased to 12 ng, additional splice variants were observed (Figure S1C red and black asterisks), which on sequencing revealed that exon 2 in *dusp-5* contains additional splice acceptor sites (data not shown). We performed all dusp-5 MO experiments at the lower end of MO concentration (6 ng) that showed effective targeting. *Actin* transcript levels are the same in both UI and MO samples (Figure S1C actin gel), indicating that MO1 selectively targets *dusp-5*. RT-PCR of a nontargeted region (exon 1) showed no differences in transcript levels between MO1 and UI samples (Figure S1C dusp-5 exon 1 gel). Dusp-5 preferentially dephosphorylates ERK in vitro,[9] and we checked endogenous phospho-Erk-1 levels in *dusp-5* knockdown (KD) embryos (Figure S1D). Dusp-5 KD embryos show higher amounts of phosphorylated Erk (Figure S1D lane MO) compared with UI embryos (Figure S1D lane UI), suggesting that knocking down dusp-5 results in loss of functional activity in dephosphorylating Erk in vivo. These results show that *dusp-5* KD in vivo results in lower transcript levels with less functional activity.

MO1-injected embryos were stained for ets1-related protein (*etsrp*), the earliest marker of angioblasts in the LPM.[19] At 6 som, *etsrp*+ cells located in the trunk regions of MO-injected embryos showed increased staining (Figure 1N,O) compared with age-matched UI embryos (Figure 1M). Quantitation shows an increase in the number of embryos that show intense *etsrp* staining after injection with 6 or 12 ng of *dusp-5* MO1 (70% and 80%) compared with UI embryos (Figure S1A, compare black bars). The trend continues at 18 som (Figure S1A). Importantly, MO2-injected embryo also shows similar defects at 6 som (Figure 1O), albeit with a lower efficacy. To check for MO effects on gastrulation, we performed an ISH for *myod*, a muscle differentiation marker, and did not notice any substantial delays in gastrulation in MO-injected embryos (Figure 1Q,R) compared with UI embryos (Figure 1P). We also checked the blood marker *gata-1* because hematopoietic cells and ECs often emerge side by side. We did not observe a difference in *gata-1*+ cell patterning in MO-injected embryos (Figure 1T,U), but a slight increase in *gata-1* staining is noticed in the blood islands (Figure 1S-U red asterisks). These results suggest that dusp-5 may affect both the hematopoietic and vascular cells during embryonic development.

Dusp-5 and snrk-1 target a common signaling pathway in angioblast development

In a previous study, we had identified a serine threonine kinase, snrk-1, which when overexpressed in ZF affects *etsrp*+ populations.[12] Here, we show that *dusp-5* KD affects the same population of cells. Based on this similarity, we investigated whether *dusp-5* and *snrk-1* target a common signaling pathway controlling angioblast development at the LPM. We performed reciprocal coinjection experiments where we coinjected *snrk-1* MO and *dusp-5* mRNA (Figure 2B) or *dusp-5* MO and *snrk-1* mRNA (Figure 2C) and stained for *etsrp* at 6 and 18 som. Until 6 som, all embryos appeared grossly normal (data not shown). At 18 som, embryos injected with *snrk-1* MO and *dusp-5* mRNA (Figure 2B) showed no difference in *etsrp*+ cell localization compared with UI embryos (Figure 2A), indicating that *snrk-1* KD is rescued by *dusp-5* overexpression. However, most embryos (Figure 2D, 80%) injected with *dusp-5* MO and *snrk-1* mRNA (Figure 2C) were severely abnormal at 18 som (Figure 2C). These embryos showed increased *etsrp*+ cells in the LPM that did not migrate to the midline as in UI (Figure 2A) or *snrk-1* MO, *dusp-5* mRNA-injected embryos (Figure 2B). These data suggest that *dusp-5* and *snrk-1* target a critical pathway in embryonic development and that *dusp-5* acts downstream or parallel to *snrk-1*.

Ectopic induction of etsrp+ angioblasts by snrk-1 is blocked by dusp-5

To investigate gain of function, we injected 75 pg of capped RNA of dusp-5 and snrk-1 alone or together and performed *ISHs* for *etsrp* at 6 and 18 som. As shown previously,[12] embryos singly injected with 75 pg of *snrk-1* mRNA showed ectopic *etsrp*+ expression along the longitudinal axis parallel to the midline and the LPM boundary of the embryo (Figure 3H bracket) at 6 som. In singly *dusp-5* mRNA-injected embryos (Figure 3D,E), an ectopic increase in *etsrp*+ cells was not as substantial along the LPM edges (Figure 3F). In double mRNA-injected 6 som embryos (Figure 3J-L), ectopic *etsrp* expression was stunted along the longitudinal (Figure 3K bracket) and lateral axes (Figure 3L asterisks), suggesting that *dusp-5* blocks *snrk-1*–induced ectopic expression of *etsrp* in the LPM. At 18 som, double mRNA-injected embryos did not show any remarkable changes in the *etsrp*+ cell population (data not shown), suggesting restored regulation of angioblast development. Quantitation (Figure 3M) shows that 60% to 80% of *snrk-1* mRNA-injected embryos showed increased *etsrp* staining along both axes of the embryo, 40% to 50% of *dusp-5* mRNA-injected embryos showed increased *etsrp* along the shorter axis but decreased *etsrp* along the longer axis, and a majority (80%-100%) of double mRNA-injected embryos displayed increased *etsrp*
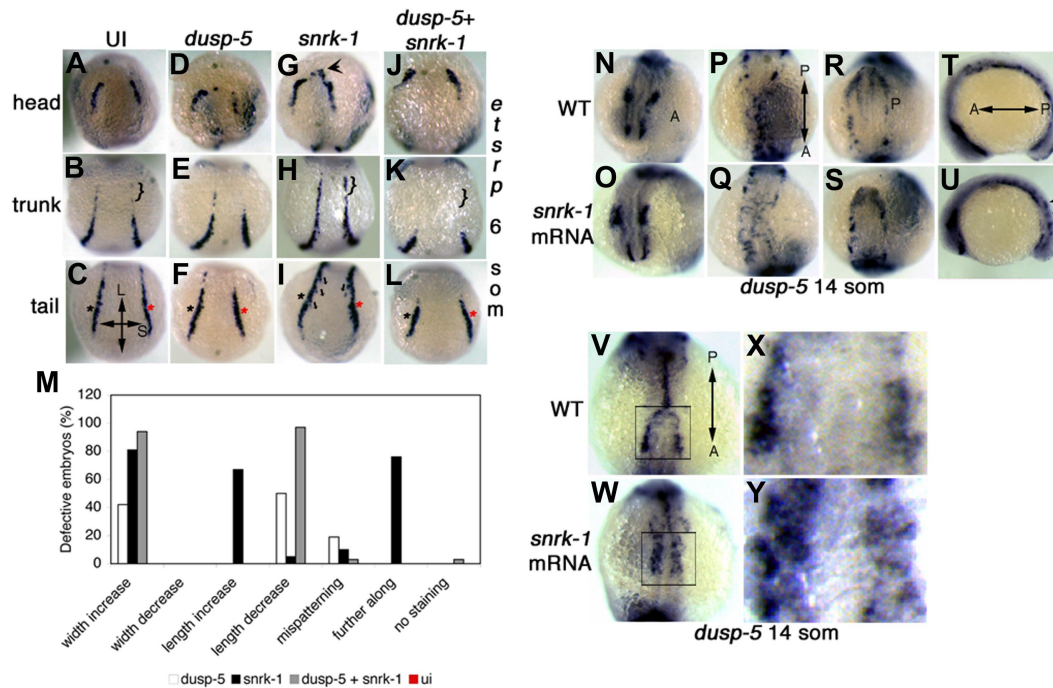
Figure 3. Snrk-1–induced ectopic induction of *etsrp*+ angioblasts is blocked by *dusp-5*. (A-L) *etsrp* ISHs at 6 som. (A-J, B-K, and C-L) *etsrp*+ head, trunk, and tail populations, respectively. *Dusp-5* mRNA-injected embryos (D-F), compared with UI embryos (A-C), show decreases in the length and width of the tail *etsrp*+ population (compare red asterisk in panels C and F). *Snrk-1* mRNA-injected embryos show increases in all 3 *etsrp*+ populations (compare black arrow in panel G, bracket in panel H, and asterisks in panel I). Furthermore, the direction of *etsrp*+ cell migration (black arrows in panel I) is toward the midline. Embryos injected with both *dusp-5* and *snrk-1* mRNA (J-L) show the most dramatic decrease in *etsrp*+ populations across the longitudinal and short axes of the embryo. (M) Quantification of the different phenotypes observed in UI (ui, n = 25), single mRNA-injected (snrk-1, n = 21 or dusp-5, n = 26), or combination-injected embryos (snrk-1 + dusp-5, n = 31). (N-U) *dusp-5* ISH embryos in UI wild-type (WT) (N-T) and *snrk-1* mRNA-injected embryos (O-U) at 14 som. High power images of the boxed region in panel V (WT) and panel W (*snrk-1* mRNA) are shown in panels X and Y, respectively. (N,O) Minimal differences in *dusp-5* ISH in the head. (P) Properly migrated *dusp-5*+ cells that make a distinguishable "Y"-shaped pattern; this pattern is not seen in the trunk region of *snrk-1* mRNA-injected embryos (Q). Little difference is noted in the tail region between WT (R) and *snrk-1* mRNA-injected embryos (S). Further, *snrk-1* mRNA-injected embryos (U) appear further along developmentally compared with WT embryos (T) in the lateral view, and *dusp-5*+ cells are observed on a different plane in *snrk-1* mRNA-injected embryos (black arrows in panel U). In high-power images of *snrk-1* mRNA-injected embryos (Y), the patterning of *dusp-5*+ cells is affected compared with similar regions in WT embryos (X), and they also appear closer to the midline in *snrk-1* mRNA-injected embryos with more diffuse distribution. "L" and "S" labels in panel C denote longitudinal and short axes, respectively, for panels A to L. "A" and "P" labels in panels N, P, R, T, and V denote the direction of the anterior-posterior axis in corresponding panels (N-Y).

expression along the shorter axis and decreased *etsrp* along the longer axis.

To determine whether ectopic induction was specific to *etsrp*+ angioblasts, we performed an ISH with the endothelial marker *flk* at 14 som (Figure S2C-I) and 18 som (Figure S2D-J) on mRNA-injected embryos and found that *flk*+ populations are also affected. UI embryos at 14 som (Figure S2C) show a characteristic Y-shaped *flk*+ angioblast migration pattern (Figure S2C white arrows). In both *dusp-5* (Figure S2E) and *snrk-1* (Figure S2G) mRNA-injected embryos, this migration pattern is affected. In *snrk-1* mRNA-injected embryos (Figure S2G), the overall extent of *flk* staining is increased, suggesting that ectopic induction of *flk*+ cells occurs. Interestingly, in *dusp-5* and *snrk-1* mRNA-coinjected embryos, the Y-shaped *flk*+ angioblast pattern is restored (Figure S2I black arrows). At 18 som, angioblasts have migrated to the midline in UI embryos (Figure S2D white asterisk). *Flk*+ angioblasts in the midline are affected in *snrk-1* mRNA-injected 18 som embryos (Figure S2H), whereas *dusp-5* mRNA-injected 18 som embryos (Figure S2F) show little to no change. In the case of double mRNA-injected embryos (Figure S2J), the *flk*+ angioblast patterning appears intermediate between the phenotypes of UI and single mRNA-injected embryos. These results argue that *snrk-1* acts upstream or parallel to *dusp-5* in a signaling pathway necessary for maintaining angioblasts along the length and breadth of the embryo.

Snrk-1 overexpression alters migration of *dusp-5*+ angioblasts in vivo

To investigate whether *snrk-1* overexpression affects the *dusp-5*+ angioblasts, we injected capped *snrk-1* mRNA and performed *dusp-5* ISHs at 14 som (Figure 3N-U). In the head at 14 som, no difference is observed in *dusp-5*+ angioblasts in WT (Figure 3N) vs *snrk-1* mRNA-injected (Figure 3O) embryos. In the trunk of 14 som UI embryos (Figure 3P), *dusp-5*+ angioblasts have migrated to the midline, but in *snrk-1* mRNA-injected embryos, this migration is affected (Figure 3Q), most evident when observed in lateral view (Figure 3U); *dusp-5*+ angioblasts of *snrk-1* mRNA-injected embryos are more dorsal (Figure 3U black arrows) than that of their uninjected counterparts (Figure 3T). Moreover, in high power images of the trunk region, *snrk-1* mRNA-injected embryos (Figure 3Y) clearly show mispatterning of *dusp-5*+ cells, which appear closer to the midline than those in UI (Figure 3X) embryos. The increased number of *dusp-5*+ cells in the trunk of *snrk-1* mRNA-injected embryos may reflect ectopic induction or altered migration of angioblasts. In both the head and tail, *dusp-5*+ angioblasts are not affected in *snrk-1* mRNA-injected embryos (Figure 3S) compared with UI embryos (Figure 3R). Previously,[12] we showed that *snrk-1* mRNA-injected embryos showed altered migration of *etsrp*+ cells to the midline. Given the current study, these results suggest that *dusp-5*+ *etsrp*+ angioblasts exist in the
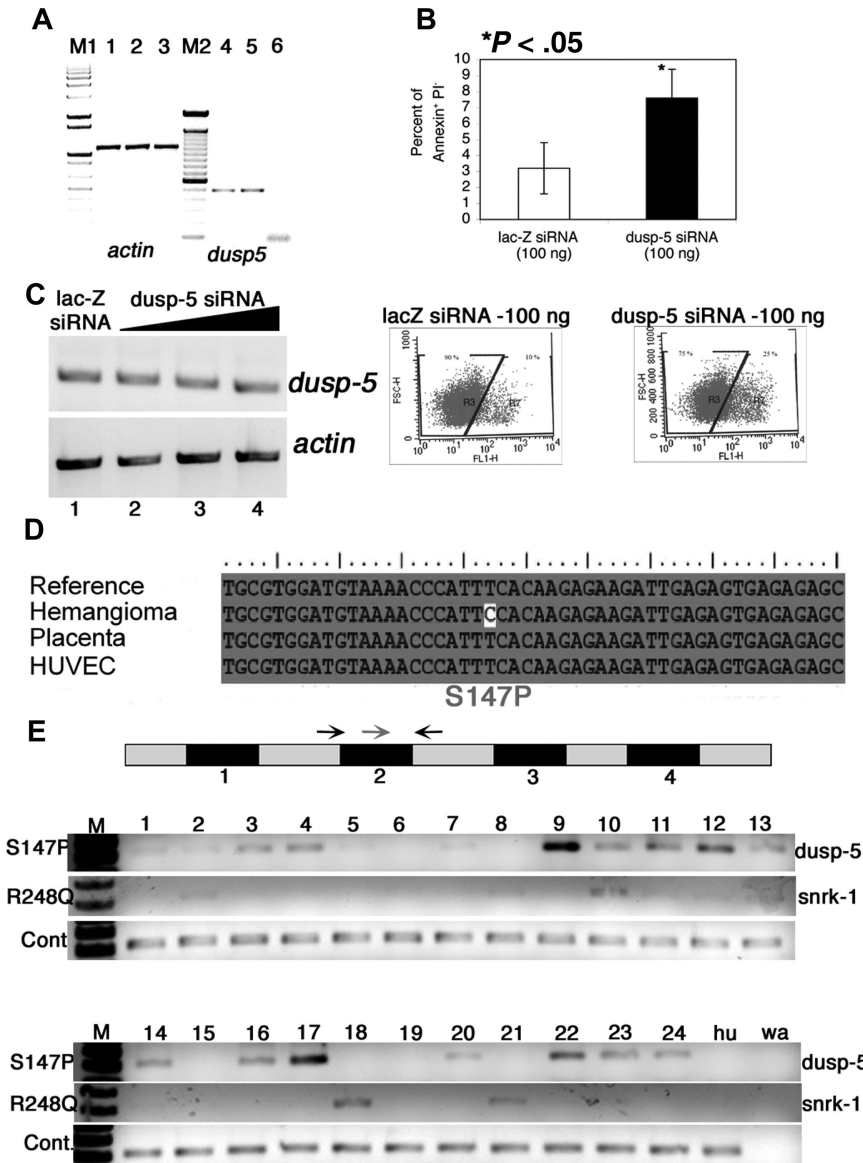
Figure 4. Dusp-5 knockdown in vitro and mutation analysis of vascular anomaly patient samples. (A) RT-PCR for *actin* (lanes 1-3) and *dusp-5* (lanes 4-6) transcripts from UI (lanes 1 and 4), *lac-Z* siRNA (lanes 2 and 5), and *dusp-5* siRNA-transfected (lanes 3 and 6) ECs. M1 indicates 1-kb DNA ladder marker; M2, 100-bp DNA ladder marker. (B) Percentage of apoptotic HUVECs (annexin V$^+$ and PI$^-$) 8 hours after transfection with 100 ng each of *lac-Z* and *dusp-5* siRNA. The data are compiled from 4 independent experiments, and the error bars represent SEM. The dot plots indicating the gates and the percentage of annexin V–fluorescein isothiocyanate$^+$ cells in *lac-Z* and *dusp-5* siRNA samples. *P < .05 between sample groups. (C) RT-PCR for *dusp-5* and *actin* transcripts from hemangioma templates. The black triangle indicates increasing concentrations of *dusp-5* siRNA (lane 2, 100 ng; lane 3, 250 ng; lane 4, 500 ng) transfected into ECs, *lacZ* siRNA (lane 1, 500 ng). No change in *dusp-5* transcript levels is noted across samples. (D) Mutation in the *dusp-5* coding sequence identified only in the hemangioma sample and not from HUVEC or placenta tissue compared with the sequence of NCBI Gene Id 1847. (E) Exon-intron structure of *dusp-5* in the genome. The numbers below the black box indicate exons. The gray boxes represent untranslated or intron sequences. Arrows indicate primers used for genomic PCR amplification. The red arrow indicates the mutated forward primer in exon 2; black arrow, the normal forward primer. The S147P PCR gel shows amplification resulting from the *dusp-5* mutation specific red primer and the *dusp-5* black reverse primer. The R248Q gel shows amplification resulting from the *snrk-1* mutation-specific primer and the *snrk-1* reverse primer. The wild-type (WT) gel shows amplification resulting from the *dusp-5* normal forward and reverse primers. The Hu lane contains DNA from HUVEC cells, and the wa lane contains a water control with no genomic DNA in the PCR.

LPM, and *snrk-1* works upstream in the signaling pathway that directs angioblast migration to the midline.

Dusp-5 knockdown in vitro causes endothelial cell apoptosis

To investigate *dusp-5* loss of function in vitro, we created siRNA using the Dicer method[20] to KD endogenous *dusp-5* transcripts in ECs. To demonstrate siRNA targeting of endogenous *dusp-5* transcripts, RT-PCR was performed with *dusp-5*-specific primers on total RNA isolated from untransfected and lac-Z or *dusp-5* siRNA-transfected ECs (Figure 4A lanes 4-6). Endogenous *dusp-5* transcripts are knocked down in *dusp-5* siRNA-transfected cells (Figure 4A lane 6). RT-PCR for *actin* shows equal amounts of input RNA in all samples (Figure 4A lanes 1-3).

We investigated the effect of *dusp-5* KD on proliferation, migration, and apoptosis. In proliferation assays, we observed increased cell death in *dusp-5* siRNA-transfected ECs and therefore investigated whether apoptosis is induced in these cells. We assessed apoptosis using the annexin V-fluorescein isothiocyanate assay.[21,22] *Dusp-5* siRNA-transfected ECs show at least a 2-fold increase in apoptosis compared with *lac-Z* siRNA-transfected cells 8 hours after transfection (Figure 4B). These apoptosis data provide

a simple mechanistic explanation for *dusp-5*'s function in vivo; ECs are unable to survive without *dusp-5*. We also performed adhesion assays and noticed a difference in adhesion of *dusp-5* siRNA KD cells and *lac-Z* siRNA-transfected cells on fibronectin (Figure S2K compare black bars; P < .05) but not laminin. Because *dusp-5* KD ECs are dying, it is unclear whether the lack of adhesion is primary or secondary to apoptosis.

Many human vascular anomaly specimens show mutations in *dusp-5* and/or *snrk-1*

While studying the in vitro function of *dusp-5*, we fortuitously used RNA from a human infantile hemangioma sample to prepare siRNA. The dicer siRNA generated from this infantile hemangioma sample failed to target endogenous *dusp-5* transcripts in HUVECs (Figure 4C compare lanes 2-4 with lane 1), which were previously targeted when siRNA was generated from a HUVEC template (Figure 4A compare lanes 4-6). To explain this discrepancy, we hypothesized that the cDNA template used for generating siRNA from the hemangioma sample contained a mutation. Sequencing of the *dusp-5* coding regions in the hemangioma sample resulted in identification of 2 mutations. One of the mutations is a T–C

substitution resulting in a serine to proline change at amino acid 147 (S147P; Figure 4D) that would probably make the protein unstable. This mutation was not found in *dusp-5* cDNA isolated from human placenta or HUVEC cells.

To screen for the S147P mutation in a larger number of samples, we designed a diagnostic PCR test (Figure S3A) in which the forward primer (Figure 4E gray arrow) contains the mutated C residue at the 3′ end and the reverse primer (Figure 4E reverse black arrow) corresponds to genomic DNA. We hypothesized that the PCR would only work if the mutation was present in the patient samples. As a control, we included a second forward primer without the mutated 3′ C residue (Figure 4E left black arrow). Twenty-four patient samples representing a variety of vascular anomalies were tested in a blinded fashion. PCR for both sets of primers (S147P and WT) revealed that 17 of 24 samples screened contained the mutated dusp-5 sequence (Figure 4E S147P PCR). All samples (24 of 24) excluding the control water sample (Figure 4E wa lane) amplified the *dusp-5* fragment flanking exon 2, demonstrating that roughly equivalent amounts of genomic DNA were present in each reaction (Figure 4E WT gel). The HUVEC controls only showed the normal *dusp-5* band (Figure 4E hu lane).

The PCR products were sequenced from 3 patient samples (9, 17, and 24), and the S147P *dusp-5* mutation was confirmed (Figure S3B). Some samples (Figure 4E lane 9) showed more PCR product than others, but the significance of this finding in terms of disease type is unclear, perhaps reflecting percentage of cells in the tissue carrying the mutant sequence. Unveiling the diagnoses of each of the tested samples revealed that the *dusp-5* S147P mutation was found in different types of vascular malformations and tumors, including lymphatic (6 of 8), arteriovenous (3 of 4), and venous malformations (3 of 5), and infantile hemangiomas (1 of 3). Although the sample sizes per specific clinicopathologic entity is small, these data indicate that altered *dusp-5* genomic sequences representing either polymorphism or somatic mutation are present in a variety of vascular anomalies, strongly suggesting that dusp-5 pathway components may play an important role in these vascular conditions. Before the PCR-based approach, we attempted a mutation screen by making cDNA from each sample and sequencing the clones. However, the mutation detection frequency was extremely low (1 of 17 clones; data not shown). This result and the identification of mutations in several samples by the PCR diagnostic approach suggest that perhaps only a small population of cells in each patient sample carry this aberrant genomic DNA and that this mutation is not a polymorphism that would be expected in all of the patient's cells. We also screened for the S147P mutation in tonsil tissue from 10 randomly selected patients without vascular anomalies (Figure S3C) and did not identify the mutation in any of them. Collectively, these results suggest that the *dusp-5* mutation in vascular anomalies is somatic in origin, pending parallel assessment of unaffected tissue from patients with these disorders.

Given the coordinated effects of *snrk-1* and *dusp-5* in vascular development, we also checked for mutations in *snrk-1* in the 24 vascular anomaly specimens. From our initial screen of 6 samples, we identified one patient with 3 mutations: a R248Q mutation in the kinase domain and S259Y and D192G mutations (Figure S3D). This patient also harbored the S147P *dusp-5* mutation. We focused on the R248Q mutation because it occurs in the kinase domain and alters the protein's charge. We extended the PCR diagnostic approach to *snrk-1* and found that 8 of 24 samples carried the *snrk-1* R248Q mutation. We sequenced the PCR bands from samples showing strong amplification (10, 18, and 21) and confirmed the mutation (Figure S3E, yellow highlight). In addition,

we noticed 2 trends (Figure 4E, R248Q PCR). First, for the most part, patients carrying the *snrk-1* R248Q mutation also carry the *dusp-5* S147P mutation (6 of 8). Second, the majority of *snrk-1* R248Q mutations were found in lymphatic or venous malformation samples (5 of 8). Lymphatic endothelial populations originate from a venous lineage,[23] and *snrk-1* KD in ZF leads to artery versus vein specification defects.[12] Together, these results suggest that the *dusp-5* and *snrk-1* signaling pathway could be critically disrupted in specific categories of vascular anomalies.

Discussion

Dual specific phosphatases belong to a unique class of proteins that counteract MAPKs. Although several members of the MAPK pathway are involved in cardiovascular pathophysiology and development,[5] relatively little is known about counteracting phosphatases in these processes. This study identifies a member of the dual specific phosphatase family, Dusp-5, which functions in vascular development in vertebrates.

We report 3 important findings. First, Dusp-5 is a vascular-specific phosphatase that maintains angioblast numbers in the LPM and works in concert with a serine threonine kinase, Snrk-1. Second, Dusp-5 and Snrk-1 target a signaling pathway critical for embryonic development. Third, somatic mutations in *dusp-5* and *snrk-1* underscore the importance of this pathway in human pathophysiology.

Before our report, 2 independent groups identified *dusp-5* as a vascular-specific gene in microarray analyses of *cloche*, a cardiovascular mutant in ZF.[10,11] Our report confirms *dusp-5*'s vascular function. *Dusp-5* is expressed in LPM cells that are specified to become angioblasts as early as 8 som. Angioblasts migrate to the midline between 12 and 16 som, and *dusp-5* expression is noted in angioblasts at the midline at 14 som. It is unclear whether *dusp-5* has a role in migrating angioblasts because ISH analysis may not be sufficiently sensitive to detect these cells. Once angioblasts reach the midline at 18 som, they coalesce and are specified to become either an artery or vein. *Dusp-5* continues to be expressed in the midline at 18 som and is expressed in the axial vessels until 36 hpf. Functional analyses show that, as early as 6 som, *etsrp*[+] angioblasts are affected by both gain and loss of *dusp-5*, suggesting that *dusp-5* is involved in angioblast maintenance. This argument is based on the fact that *dusp-5* KD in vitro causes apoptosis of differentiated ECs and is based on the assumption that the functional mechanism for a given gene in endothelial precursors and differentiated ECs is conserved. Our findings that *snrk-1* KD causes migration defects in HUVECs and in *etsrp*[+] angioblasts in ZF further bolster this assumption.[12]

We initiated the current study to investigate whether *dusp-5*, a candidate gene identified in 2 independent microarray studies[10,11] shows vascular specific function. We obtained similar results of altered *etsrp*^{+} cells along the LPM in *dusp-5* LOF embryos as seen previously for *snrk-1* LOF,[12] suggesting that *dusp-5* and *snrk-1* may function together during embryonic vascular development. *Snrk-1* overexpression ectopically induces *etsrp*[+] angioblasts along the LPM, and this induction does not occur in the presence of *dusp-5*. It is worthwhile to note that ectopically induced angioblasts in *snrk-1* mRNA-injected embryos are undergoing apoptosis.[12] These data suggest that *snrk-1* and *dusp-5* control angioblast populations by ensuring survival of the appropriate number for migration to the midline. This interpretation is further strengthened by results from reciprocal loss and gain-of-function experiments

with *snrk-1* and *dusp-5*. In *snrk-1* overexpression embryos lacking *dusp-5*, most embryos are normal until 6 som, but by 18 som, more than 90% of embryos die. One explanation for this result is that at 6 som in *snrk-1* overexpression embryos, the number of *etsrp*[+] angioblasts has increased, and these angioblasts are eventually dying.[12] Removal of *dusp-5* causes this process to accelerate. In the reverse situation where *snrk-1* is removed and *dusp-5* is overexpressed, increasing *dusp-5* expression causes these cells to survive, and embryos look normal at 18 som. These experiments imply that a signaling pathway in which *snrk-1* works upstream of *dusp-5* is critical for embryonic development after 6 som. Further detailed marker analysis between 6 and 18 som is necessary before determining the exact stage in the angioblast development that is affected by the snrk-1–dusp-5 signaling axis.

The identification of somatic mutations in *dusp-5* and *snrk-1* places these genes in a disease context. MAPK activation occurs by dual phosphorylation of tyrosine and threonine residues in their activation loops. Dual specific tyrosine phosphatases presumably counteract this activation. Aberrant activation of MAPKs or DUSPs is associated with human disorders, such as cancer, diabetes, or autoimmune conditions.[24,25] Our studies suggest that the pathogenesis of vascular malformations may result from aberrant *dusp-5* and *snrk-1* signaling. Reactive oxygen species has been reported to inhibit the catalytic activity of specific tyrosine phosphatases (dusp-1) in an angiomyolipoma cell model[26] and treatment using nicotinamide adenine dinucleotide phosphate (reduced form) oxidase (Nox) inhibitors abolished hemangioma growth in vivo via blockage of angiopoietin-2 production.[27]

It makes sense that mutations in *dusp-5* and *snrk-1* play an integral role in these conditions because both genes work together to maintain vascular precursors. We have observed *dusp-5* mutations, but not *snrk-1* mutations, in infantile hemangioma. Infantile hemangioma is the most common tumor of infancy and is characterized by initial rapid growth and eventual involution. Loss of *dusp-5* function may promote vascular precursor cell migration or growth during the tumor's proliferative phase by removing *dusp-5*'s blockade of *snrk-1* signaling. *Dusp-5* KD embryos show high ERK levels (Figure S1D), *erk* KD embryos show critical migration defects during gastrulation,[28] and the ERK pathway critically regulates distinct gene sets in embryogenesis.[29] Alternatively, *dusp-5* mutations might promote endothelial apoptosis during involution. The coordination of *dusp-5* and *snrk-1* in regulating angioblast numbers and migration in the ZF suggest that somatic mutations in either gene might cause or modulate congenital vascular malformations.

We found *dusp-5* mutations in 1 of 3 infantile hemangioma specimens and in 12 of 17 vascular and lymphatic malformations. All *dusp-5* mutations observed in vascular anomaly specimens were not conservative substitutions, but ones that would alter protein structure, charge, and, in turn, function. Thus, we conclude that alterations in Dusp-5 may be associated with a variety of vascular abnormalities. Interestingly, the *snrk-1* mutations observed were found exclusively in venous and lymphatic malformations, suggesting that loss of *snrk-1* expression influences these vascular anomalies. The lymphatic vascular system develops from the venous system,[23] and venous and lymphatic malformations are often mixed, as was the case in 5 of 8 tissue specimens containing a *snrk-1* mutation.

Our data suggest that somatic mutations in *snrk-1* and *dusp-5* may be found in a minority of cells present in affected tissues. This interpretation is supported by our diagnostic PCR test in which different amounts of mutated genomic DNA were amplified in different specimens despite equal levels of normal PCR product. This also argues against the presence of germline mutations in *snrk-1* and *dusp-5*. We must determine by laser capture microdissection which cells within the affected tissues contain mutated DNA. Based on high expression of *snrk-1* in hemangioma tissue (data not shown), we hypothesize that the mutated gene is harbored in ECs. However, its presence in other supporting cells, such as mesenchyme,[30] cannot be excluded.

Vascular anomalies of infancy and childhood, despite their "benign" nature, present major medical challenges, both diagnostically and in terms of clinical management. Current therapies are limited in efficacy and have significant complications. It is our hope that identification of specific mutations in the lesions of individual patients will lead to better prediction of biologic behaviors and outcomes and to the development of effective, targeted therapies. To better assess the clinical relevance of *snrk-1* and *dusp-5* mutations, we must analyze tissues from more patients with vascular anomalies and correlate our results with clinical presentations.

In conclusion, we have identified a novel-signaling axis involving a kinase, *snrk-1*, and a phosphatase, *dusp-5*, which play important roles in embryonic vascular development and are mutated in vascular anomalies in human patients.

Acknowledgments

Authorship

Contribution: K.P., C.Z.C., M.K.G., P.E.N., and R.R. designed research; K.P., C.Z.C., G.V.S., M.K.G., M.A.H., and K.L. performed research; C.Z.C., K.P., M.K.G., G.V.S., P.E.N., and R.R. analyzed the data; and R.R. and P.E.N. wrote the paper.

Conflict-of-interest disclosure: The authors declare no competing financial interests.

Correspondence: Ramani Ramchandran, Department of Pediatrics, CRI Developmental Vascular Biology Program, Medical College of Wisconsin, 8701 Watertown Plank Road, Milwaukee, WI 53226; e-mail: rramchan@mcw.edu.

References

1. Ferrara N. Role of vascular endothelial growth factor in physiologic and pathologic angiogenesis: therapeutic implications. Semin Oncol. 2002;29:10-14.

2. Raman M, Chen W, Cobb MH. Differential regulation and properties of MAPKs. Oncogene. 2007; 26:3100-3112.

3. Regan CP, Li W, Boucher DM, Spatz S, Su MS, Kuida K. Erk5 null mice display multiple extraembryonic vascular and embryonic cardiovascular defects. Proc Natl Acad Sci U S A. 2002;99:9248-9253.

4. Yang J, Boerm M, McCarty M, et al. Mekk3 is essential for early embryonic cardiovascular development. Nat Genet. 2000;24:309-313.

5. Feuerstein GZ, Young PR. Apoptosis in cardiac diseases: stress- and mitogen-activated signaling pathways. Cardiovasc Res. 2000;45:560-569.

6. Jeffrey KL, Camps M, Rommel C, Mackay CR. Targeting dual-specificity phosphatases: manipulating MAP kinase signalling and immune responses. Nat Rev Drug Discov. 2007;6:391-403.

7. Arbiser JL, Weiss SW, Arbiser ZK, et al. Differential expression of active mitogen-activated protein

kinase in cutaneous endothelial neoplasms: implications for biologic behavior and response to therapy. J Am Acad Dermatol. 2001;44:193-197.

8. North PE, Waner M, Buckmiller L, James CA, Mihm MC Jr. Vascular tumors of infancy and childhood: beyond capillary hemangioma. Cardiovasc Pathol. 2006;15:303-317.

9. Kwak SP, Dixon JE. Multiple dual specificity protein tyrosine phosphatases are expressed and regulated differentially in liver cell lines. J Biol Chem. 1995;270:1156-1160.

10. Qian F, Zhen F, Ong C, et al. Microarray analysis of zebrafish cloche mutant using amplified cDNA and identification of potential downstream target genes. Dev Dyn. 2005;233:1163-1172.

11. Sumanas S, Jorniak T, Lin S. Identification of novel vascular endothelial-specific genes by the microarray analysis of the zebrafish cloche mutants. Blood. 2005;106:534-541.

12. Chun CZ, Kaur S, Samant GV, et al. Snrk-1 is involved in multiple steps of angioblast development and acts via notch signaling pathway in artery-vein specification in vertebrates. Blood. 2008 Aug 22. [Epub ahead of print].

13. Westerfield M. The Zebrafish Book, 4th ed. Eugene, OR: University of Oregon Press; 2000.

14. Kimmel CB, Ballard WW, Kimmel SR, Ullmann B, Schilling TF. Stages of embryonic development of the zebrafish. Dev Dyn. 1995;203:253-310.

15. Yeo SY, Little MH, Yamada T, et al. Overexpression of a slit homologue impairs convergent extension of the mesoderm and causes cyclopia in embryonic zebrafish. Dev Biol. 2001;230:1-17.

16. Chan J, Bayliss PE, Wood JM, Roberts TM. Dissection of angiogenic signaling in zebrafish using a chemical genetic approach. Cancer Cell. 2002; 1:257-267.

17. Fouquet B, Weinstein BM, Serluca FC, Fishman MC. Vessel patterning in the embryo of the zebrafish: guidance by notochord. Dev Biol. 1997; 183:37-48.

18. Zhong TP, Childs S, Leu JP, Fishman MC. Gridlock signalling pathway fashions the first embryonic artery. Nature. 2001;414:216-220.

19. Sumanas S, Lin S. Ets1-related protein is a key regulator of vasculogenesis in zebrafish. PLoS Biol. 2006;4:e10.

20. Hammond SM. Dicing and slicing: the core machinery of the RNA interference pathway. FEBS Lett. 2005;579:5822-5829.

21. Reutelingsperger CP, van Heerde WL. Annexin V, the regulator of phosphatidylserine-catalyzed inflammation and coagulation during apoptosis. Cell Mol Life Sci. 1997;53:527-532.

22. van Engeland M, Nieland LJ, Ramaekers FC, Schutte B, Reutelingsperger CP. Annexin V-affinity assay: a review on an apoptosis detection system based on phosphatidylserine exposure. Cytometry. 1998;31:1-9.

23. van der Putte SC. The early development of the lymphatic system in mouse embryos. Acta Morphol Neerl Scand. 1975;13:245-286.

24. Alonso A, Sasin J, Bottini N, et al. Protein tyrosine phosphatases in the human genome. Cell. 2004; 117:699-711.

25. Chang L, Karin M. Mammalian MAP kinase signalling cascades. Nature. 2001;410:37-40.

26. Boivin B, Zhang S, Arbiser JL, Zhang ZY, Tonks NK. A modified cysteinyl-labeling assay reveals reversible oxidation of protein tyrosine phosphatases in angiomyolipoma cells. Proc Natl Acad Sci U S A. 2008;105:9959-9964.

27. Perry BN, Govindarajan B, Bhandarkar SS, et al. Pharmacologic blockade of angiopoietin-2 is efficacious against model hemangiomas in mice. J Invest Dermatol. 2006;126:2316-2322.

28. Krens SF, He S, Lamers GE, et al. Distinct functions for ERK1 and ERK2 in cell migration processes during zebrafish gastrulation. Dev Biol. 2008;319:370-383.

29. Krens SF, Corredor-Adamez M, He S, Snaar-Jagalska BE, Spaink HP. ERK1 and ERK2 MAPK are key regulators of distinct gene sets in zebrafish embryogenesis. BMC Genomics. 2008;9: 196.

30. Fong GH, Zhang L, Bryce DM, Peng J. Increased hemangioblast commitment, not vascular disorganization, is the primary defect in flt-1 knock-out mice. Development. 1999;126:3015-3025.